



Journal of Advanced Research in Fluid Mechanics and Thermal Sciences

Journal homepage:

https://semarakilmu.com.my/journals/index.php/fluid_mechanics_thermal_sciences/index

ISSN: 2289-7879



Assessment of the Effect of using a Magnetic Field on a Single Slope Solar Still Performance Integrated with an External Condenser Unit

Fatima Alzahraa Adnan^{1,*}, Hassanain Ghani Hameed¹, Zaid Maan Hasan Al-Dulaimi¹, Eliza M. Yusup²

¹ Department of Power Mechanics Engineering, Technical Engineering College / Al-Najaf, Al-Furat Al-Awsat Technical University (ATU), Najaf, 31001, Iraq

² Faculty of Mechanical and Manufacturing Engineering, University Tun Hussein Onn Malaysia, 86400 Parit Raja, Johor, Malaysia

ARTICLE INFO

Article history:

Received 13 August 2024

Received in revised form 15 November 2024

Accepted 25 November 2024

Available online 10 December 2024

Keywords:

Solar still; magnetic field; external condenser; solar distillation

ABSTRACT

As population density rises, the need for potable water grows. Solar distillation is the method of transforming briny water into drinkable water. We use solar desalination to desalinate untreated water. People commonly apply the desalination process to obtain pure water using solar stills. The primary classifications of solar stills are active and passive. This work aims to boost productivity by experimentally implementing the condensation and evaporation processes inside the still. To achieve this, we incorporate a magnetic field and an external condenser into the traditional distillation apparatus. The findings indicate that the outputs of the traditional solar still, the traditional solar still with a magnetic field and an external condenser (CSS-MACO), and the traditional solar still with a magnetic field (CSS-MAG) are 3.800, 5.210, and 5.800 L/m²/day, respectively. Therefore, the utilization of a magnetic field results in a 52.63% increase in productivity, while the combination of a magnetic field and an external condenser leads to a 37.10% improvement, compared to the typical solar still. From a cost analysis perspective, incorporating a magnetic field alongside a conventional solar still is the most cost-effective choice in terms of the total expense per liter of pure water. To be more specific, the cost is 0.016 USD, which is 30.43% lower than the CSS cost.

1. Introduction

The current challenge for society is to meet the significant demand for freshwater, which is rapidly decreasing due to exponential population growth and rapid urbanization. The solar still is a cost-effective method to acquire potable water, as it relies exclusively on the copious and freely available energy from the sun for its functioning [1,2]. Based on their working mode, we can categorize solar stills into two main categories: active and passive. Passive solar stills involve thermal treatment and distillation processes occurring within the enclosed still, while active stills have a supplementary heating resource to elevate the temperature of the water in the basin or enhance the

* Corresponding author.

E-mail address: fatima.ms.etcn9@student.atu.edu.iq

<https://doi.org/10.37934/arfmts.125.1.139157>

pace of evaporation/condensation processes. For instance, you can combine a still with an external condenser, solar pond, solar collector, or excess thermal energy from a power plant or industrial facilities [3,4].

CSS is the most widely spread kind due to its cost-effectiveness, ease of production, availability of raw materials, and user-friendly character. Due to the system's low productivity, the academics prioritized improving its essential operations. This included upgrading the condensation or the evaporation process, or both [5].

Abdulridha *et al.*, [5] conducted an experiment to see if they could improve the evaporation process in a still using both flat plate solar collectors and finned tube solar collectors, as well as regular stills. This led to more output. The results demonstrate that the amounts of water generated by the traditional solar still, the solar still with finned tubes solar collector, and the solar still with a flat plate solar collector are 2.886, 4.766, and 3.853 liters per square meter per day, respectively. Hence, the utilization of flat plate and finned tube solar collectors leads to a significant boost in production, with a 65.12% and 33.49% increase, respectively, compared to conventional solar stills. They performed a cost analysis on three different solar still models, specifically targeting a production of 1 liter. The results suggest that the classic still with finned tube collector is the most cost-effective option.

Kabeel *et al.*, [6] explored the use of red bricks covered with cement in a modified single-sloped solar-powered still to enhance purified water generation. Compared to a traditional solar still, the results indicate a 34% increase in water temperature and a 45% increase in output. The altered solar distillation apparatus outperformed double slope-double basin solar stills, yielding 38.8% more. However, increasing the mass of water in the modified solar still resulted in a decrease in daily production and a higher price per liter of distilled water.

Hameed *et al.*, [7] conducted a quantitative analysis to investigate the improvement in efficiency in a single-sloped, single-basin solar-powered still. They suggested a novel design for the absorbing plate with the goal of increasing the surface area for evaporation. The absorbent base design utilizes stainless steel geometries of varying shapes and sizes to maximize their impact on solar still output. The data indicate that using a stainless-steel structure leads to an increased rate of evaporation, thereby improving the efficiency of the still. The traditional solar still's output rate was measured at 2.987 kg/m². The highest temperatures observed were 63.6 °C for the stagnant water and 54.2 °C for the inner surface of the translucent lid. The cones were utilized to achieve the maximum level of freshwater productivity, yielding a water production rate of 4.13 kg/m² and an improvement ratio of 38.2%. During this event, the highest possible temperatures recorded were 72.9 °C for the stagnant water and 61.9 °C for the internal surface of the transparent cover.

Dhivagar *et al.*, [8] examined the integration of sensible heat storage material (gravel coarse aggregate) with a single-slope solar still at Coimbatore city's weather patterns. The system achieved a maximum exergy and energy efficiency of 4.7% and 32%, respectively, for a water depth of 1 centimeter. The highest productivity of 4.21 kg /m². day was witnessed for 12 hours. The price of distilled water per liter was \$0.0618, and it took 4.3 months to recover the investment. Throughout its entire cycle, the system effectively mitigated 8.27 tons of CO₂ emissions per 1 centimeter of water depth. The depth of the water and the intensity of solar radiation mostly affect efficiency. The water quality assessment showed all samples to be potable and meeting the Bureau of Indian Standards.

Saeed *et al.*, [9] conducted a numerical investigation to analyze the efficiency of a single-slope solar still. The study involved the use of various quantities of phase change material (PCM), both with and without nanoparticles. Nanoparticles are utilized to enhance the thermal conductivity of paraffin wax. The commonly utilized paraffin wax (PCM) and Al₂O₃ (nanoparticles) combine their distinct thermal characteristics with a fusion temperature, which is the focus of the main active properties'

investigation. The numerical solution was obtained using the COMSOL 5.3 software. The results were then compared to previous studies and demonstrated a high level of agreement. The results indicated that utilizing 1 kg of phase change material (PCM) is the most effective means of enhancement. Consequently, incorporating 3 Vol.% concentration of Al_2O_3 nanoparticles dispersed in 1 kg of paraffin wax offers the potential to enhance the daily productivity of the conventional single slope solar still by approximately 20%.

In their study, Jaafar *et al.*, [10] examine the utilization of specially constructed copper pipes, which are emptied of air and have varying widths, along with variable ratios of water filling. The objective is to improve the evaporation and thermal efficiency of a solar still with a single slope. Augmenting the absorption capacity of the solar still basin plate or improving the heat transfer with raw water can amplify the proportion at which clean water is produced. Empirical studies demonstrate that the utilization of empty pipes with a diameter of 15mm and a filling ratio of 50% greatly improves the evaporation and thermal efficiency of the solar still, resulting in a notable 90.09% augmentation in the production of pure water. The findings indicate that employing evacuated pipes can significantly influence the efficiency of solar stills, and augmenting the pipe width further improves the effectiveness.

Faisal *et al.*, [11] performed an empirical study to expand the daily production of solar still. The cooling water was intermittently sprayed for 30 seconds, with varying intervals of 5 minutes, 10, 20, and 30 minutes between each succeeding spray. The current study also examined the configuration of a continuous cooling water spray. The results showed that the daily output of a typical solar still augmented by 17.5%, 27%, 14%, and 10% when combined with a cooling system operating at intervals of (30 sec/ 5 min), (30 sec/ 10 min), (30 sec/ 20 min), and (30 sec/ 30 min), respectively. The optimal pulse timing for the standard single slope solar still is 30 seconds every 10 minutes. Any longer interval between pulses has a detrimental effect on the daily production.

Al-Qasaab *et al.*, [12] conducted an experimental study on a solar distillation system that utilizes a single slope solar still integrated with a parabolic dish. A copper helical conical coil was utilized to compare the steam condensation produced by the evaporator. The study's productivity was measured at 11.45 L.day⁻¹ for freshwater with a coil condenser, and 8.2 L.day⁻¹ for freshwater without a coil condenser. The average direct sun irradiation recorded was 753.6 W.m⁻². Comparing various varieties of solar stills, particularly those that have been utilized as solar irradiance concentrators, reveals exceptional performance throughout similar periods of operation. Moreover, this system can be deemed satisfactory as it has the capability to produce purified water using readily available materials in local markets at a minimal expense. It can sufficiently fulfill the daily water requirements of at least two persons.

Rahmani *et al.*, [13] performed an empirical inquiry to examine the negative impact of the exterior condenser (EC) regarding the efficiency of the standard solar still (CSS). We can demonstrate the adverse aspect of the EC by comparing the performance of the CSS and the redesigned solar still (MSS) under identical external climate conditions. The empirical findings indicate that integrating an EC into the CSS does not consistently yield favorable results, and the current weather conditions significantly impact the performance. The positive influence of the EC is clearly demonstrated under identical external climate conditions, leading to a substantial 29% boost in MSS productivity. Severe cold or hot weather conditions have an adverse effect on productivity, resulting in a decrease of approximately 16.5% compared to the average production level. The study discovered the naturally occurring circulation mode (NC) is the main mechanism responsible for transferring mass, accounting for around 63% to 80% of the water vapor transfer towards the EC. The findings demonstrate that the MSS achieves a peak daily energy efficiency of 23.2% and a peak daily exergy efficiency of 1.9%.

Conversely, the CSS exhibits a maximum daily energy efficiency of 18.25% and a maximum daily exergy efficiency of 2.4%.

Ahmed [14] conducted a 24-hour experimental investigation over the winter, autumn, and summer seasons to examine the impact of adding passive external condensers to a solar still. Three solar stills were created, each with a single-slope, single basin design. The study found that adding the upper half of the still increased output by 15.1%, 15.08%, and 16.6% compared to the typical simple solar still. The solar still linked to the condensers experienced a production rate rise of 35.8%, 33.6%, and 30.54% during the winter, autumn, and summer seasons.

Rabhi *et al.*, [15] undertook an empirical investigation to compare the performance of different types of stills, including conventional stills, stills equipped with condensers, pin fins absorbers, and stills equipped with both condensers and pin fins absorbers. The findings indicated a noteworthy rise in water output when using pin fins absorber in conjunction with an exterior condenser, leading to an improvement in hourly solar still efficiency by 12.9%, 9.7%, and 3.1%. The external condenser had a considerable impact on water production, with the pin fins absorber exerting the most substantial influence.

Numerous researchers and experts have conducted experiments Regarding the impact of magnets on evaporated water. Their observations indicate that magnetization has a beneficial effect on the amount of water evaporation.

Holysz *et al.*, [16] conducted a thorough investigation of the impact of a modest static magnetic flux on water and electrolyte solutions for 5 minutes. The study encompassed the quantification of conductivity and the quantity of water that had undergone evaporation, which were then compared to a reference system of untreated samples. The findings of the investigation indicate that the magnetic field has a significant impact on these parameters, indicating differences in the hydrolysis shell of ions. Moreover, the study also observed that there is a direct correlation between variations in conductivity and 'scaled' functions, providing conclusive evidence that the magnetic field induces these alterations.

Dhivagar *et al.*, [17] conducted a study where they measured the exergy and energy of single-sloped solar-powered stills in a basin, fitted with rectangle and circular magnets. The results indicate that the rectangle magnet solar still (RMSS) exhausted a greater output per hour, surpassing the circular magnet solar still (CMSS) by around 5.8% and the conventional solar still (CSS) by approximately 13.7%. They measured the total output in CSS, CMSS, and RMSS to be 2.15, 2.82, and 3.15 kg/m², respectively, after reading for 12 hours. The RMSS has improved its energy efficiency by 6.9% and 4.9% compared to CSS and CMSS, respectively. The exergy efficiency recorded in RMSS has escalated to 17.2% and 3.4% compared to CSS and CMSS, respectively. The RMSS and CMSS basins experience significantly lower exergy losses compared to the CSS due to the absorption of sensible heat by magnets. According to an economic study, the estimated cost of produced water (PWC) in RMSS is 4.5% cheaper than the estimated PWC in CMSS and 22.2% less than the estimated PWC in CSS. In summary, the findings demonstrated that the performance of the solar still was much improved by the magnetization of salty water.

Rufuss *et al.*, [18] undertook an empirical examination to explore the integrated impact of latent and sensible energy storage, as well as the action of magnetization Paraffin and a new nanomaterial with strong thermal conductivity (graphite plate) were employed as latent and sensible heat storage materials, respectively. The daytime yield increased by 62% and the night-time yield increased by 235%, resulting in a total yield of 5.5 kg/m²/day. In comparison, a traditional still has a yield of 3.4 kg/m²/day. The study also examined environmental and economic factors such as emissions, CO₂ reduction efforts, and the accumulation of carbon credits. The energy matrices and water quality were examined to calculate the energy-payback time, life cycle conversion efficiency (LCCE), and

purity of desalinated water. In India, the cost of one liter of freshwater was found to be 3.7% less than that of a conventional still and 69% less than that of bottled water.

This article gives an empirical investigation on solar-powered stills with a single slope. One of the stills has a magnetic field, while the other has an external condenser in addition to the magnetic field. The aim of this investigation was to address the lack of information regarding the performance of single-basin solar-powered stills with external condensers and magnetic fields in the Iraqi atmosphere. We juxtaposed the results with those from a conventional solar still (CSS) to assess the extent of enhancement this system would exhibit when integrated with a CSS. The testing took place in Najaf, Iraq, from March 17 to May 6, 2024, at the geographical coordinates $32^{\circ} 1' 38.55''$ N and $44^{\circ} 19' 59.22''$ E, which represent the local meteorological conditions.

2. Experimental Setup

Three individual solar-powered stills were constructed to assess the effectiveness of the solar-powered distillation system in this research. One of the stills is a conventional design (CSS), while the others utilize a combination of magnetic fields, one of them integrated with an external condenser as illustrated in Figure 1. The presence of magnets into the still depending on the area ratio and the location of the magnet above and below the absorption plate.

The ratio of magnet to basin area are considered in this work and calculated as follows:

$$AR = (A_m * N_m) / A_b \quad (1)$$

where;

AR: is the area ratio

A_m : is the area of magnet (m^2)

N_m : is number of magnets

A_b : is the basin linear area (m^2)

A rectangular polystyrene container with a thickness of 4.5 cm serves as the foundation for a traditional CSS structure. The stagnant basin has a $0.4 m^2$ surface area. Using a CNC machine, we precisely cut the box at a 32° angle, aligning it with the orientation of the workplace, to form the slope. We fixed the height of the front wall at 9 cm, and the height of the back wall at 40 cm. This box has a reduced amount of leakage due to its efficient sealing and insulation. Furthermore, given that polystyrene already serves as an insulating material, insulating the bottom and sidewalls of the box is unnecessary. The bowl is fitted with a transparent cover that has a 4mm thickness and a transparency rating of 0.88. We applied a dust preventer to the gaps between the stationary object and the glass cover to prevent any particle escape into the surrounding air. We built a water-collecting channel along the lower (front) side of the still, with a width of 5 mm and a slope of 2° , to collect any accumulated water. The channel diverts the collected water into a plastic bottle. An iron galvanized sheet, coated with matte black paint to enhance its ability to absorb sunlight, has been affixed to the still basin as an absorber. This galvanized sheet has overall dimensions of 50 cm by 80 cm, with a thickness of 2 mm.

The adjusted stills follow the same proportions and construction as the CSS. Moreover, the Neodymium magnets, with specifications as in Table 1, coated with black enamel, attached the basin liner with a 10% area ratio on the top surface and a 20% area ratio on the lowest surface. This is done

to improve the evaporation process, as depicted in Figure 1 and Figure 2. In addition to the magnetic field, we integrate an external condenser into the third still.

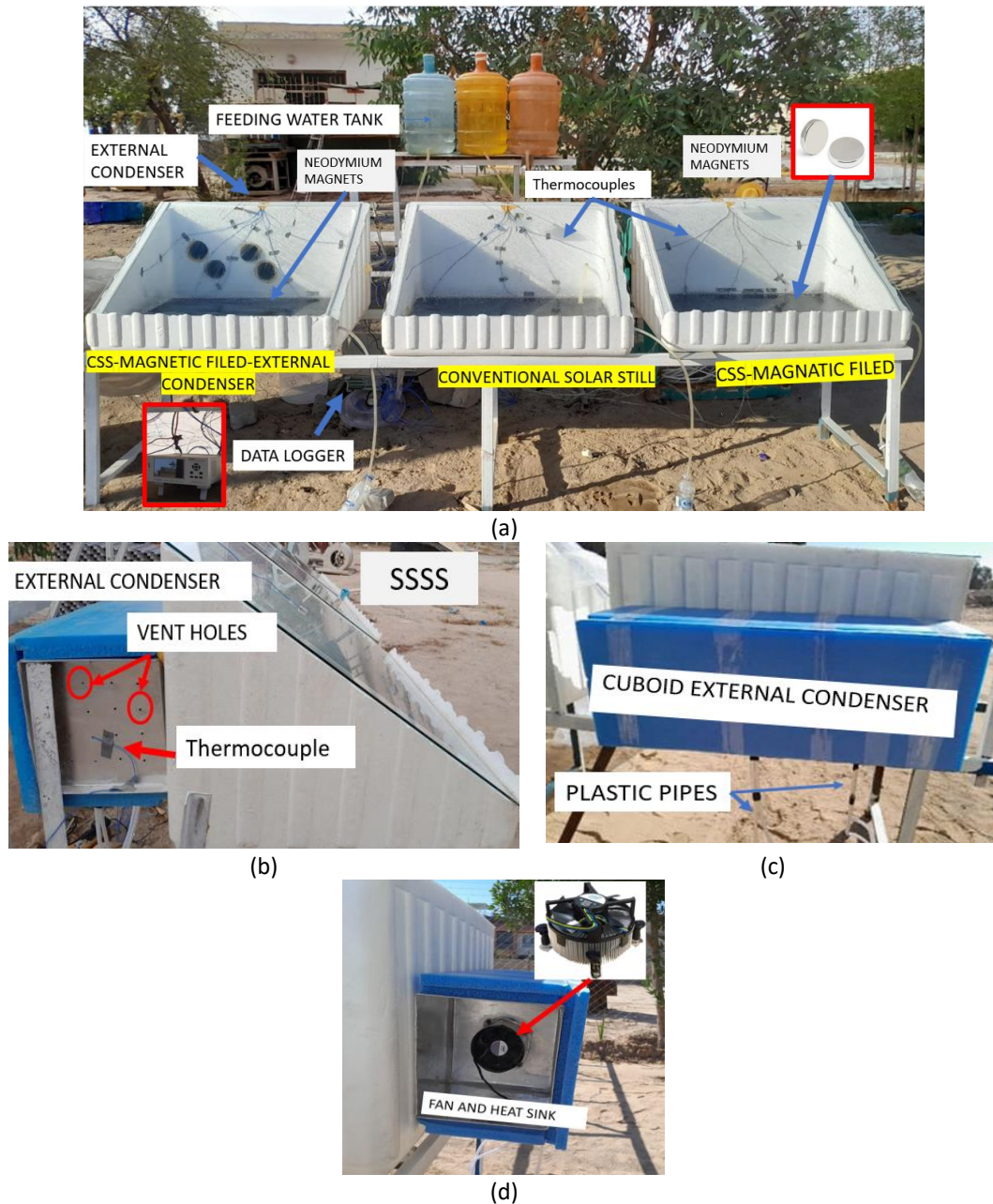


Fig. 1. (a) The experimental rigs, (b) the connection of the external condenser to the back wall of the solar still, (c) the shape of the cuboid external condenser, (d) fan and heat sink

The external condenser unit is housed in an outer cuboid chamber made of aluminum and covered with compressed insulation cork, as shown in Figure 1(b), Figure 1(c), and Figure 1(d). There are four cylindrical condensers positioned at the rear of the solar still. Each condenser has a diameter of 8 cm and a length of 20 cm. Moreover, there are water collection channels situated at the far end of the condensers. Moreover, a heat sink equips the device to ensure adequate air circulation in accordance with the compartment's temperature. The heat sink now conducts the component's generated heat, helping to maintain a lower temperature for the condenser. In order to efficiently regulate high temperatures, it is crucial to forcefully direct cool air into the heat sink. In order to accomplish this, a fan has been mounted on the uppermost portion of the heat sink, which is

positioned on the side of the Cuboid chamber. We connect the fan for active cooling to a condenser enclosure, active cooling is essential for establishing comfortable indoor conditions, albeit with significant energy use [19].

A fan is utilized to draw in cooler air from the surroundings into the enclosure, while simultaneously expelling warm air from the interior. The fan operates at a maximum rotational speed of 1800 rpm. The airflow serves the goal of enhancing the cooling process of the inside of the condenser by forcing air over a heat sink. The air from the condenser unit can be used for domestic application.

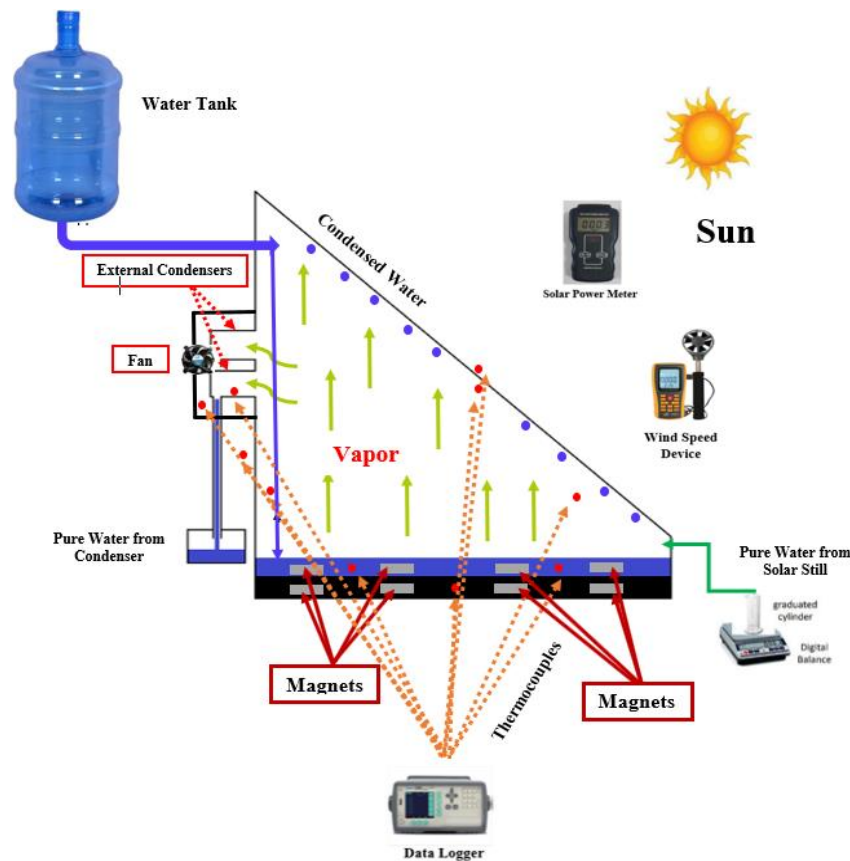


Fig. 2. Schematic diagram of the experimental rigs

Table 1

Magnet specification

Material	Shape	Grade	Thickness	Outer diameter	Density	Maximum operating temperature	Residual magnetic flux density
NdFeB	Disc	N52	3mm	10mm	7.4 g/cm ³	80 °C	1430-1480 mT

The experimental examination Occurred in Najaf, Iraq, namely at coordinates 32° 1' N and 44° 19' Measurements were taken every hour for:

The sun's rays on an hourly basis are measured by an SM206 meter that is used with an acceptable range of 0 to 1370 W/m² Figure 3 (a). The solar meter is angled similarly to the transparent cover to ensure accurate irradiation readings. We measure wind speed every hour using a GM-8902 anemometer Figure 3(b), which has a measurement range of 0 to 89 m/s. Vapor, absorbing plate, basin water, outer and inner transparent cover, inner condenser, and outlet air temperatures are recorded on an hourly basis using calibrated K-type thermocouples throughout solar stills and condenser units. CSS and CSS-MAG use seven thermocouples, while CSS-MACO requires nine. An

additional thermocouple is used to measure ambient temperature. All temperature sensors have connections with a digital data recorder (AT4532), Figure 3(c). Distilled water productivity is measured after cumulated hourly by weight balance device, Figure 3(d). Figure 4(a) and Figure 4(b) and Table 2 illustrate the exact locations of the thermocouples in the solar still and external condenser unit. Table 3 provides the specifications for the measurement equipment, including their range and accuracy. Calculate the standard uncertainty is carried out by accounting for the linear fluctuation in the equipment's data. Therefore, it is found to be $a/\sqrt{3}$, where a represents the precision of the measuring device [20].

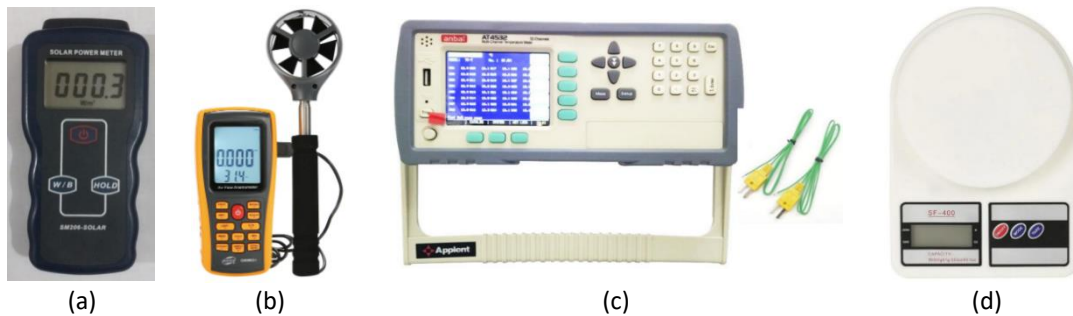


Fig. 3. (a) Solar power meter (SM206), (b) GM8902 anemometer device, (c) data logger, (d) weight balance device

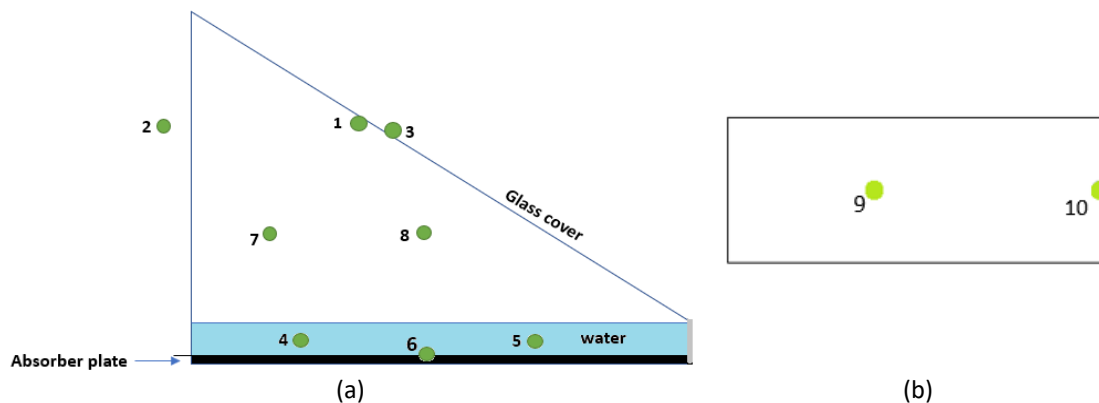


Fig. 4. The position of thermocouples in (a) solar still, (b) external condenser

Table 2
 The position of thermocouples names

Thermocouple No.	1,3	2	4,5	6	7,8	9	10
Location	Inner and outer glass surfaces	Ambient temperature	Basin water	Absorbing plate	Vapor	Inner condenser	Condenser vent hole

Table 3
 Accuracy and uncertainty for the measurement apparatus

Instruments	Accuracy	Range	Standard Uncertainty
Thermocouples	$\pm 1.2 \text{ }^\circ\text{C}$	0 – 270 $^\circ\text{C}$	0.692 $^\circ\text{C}$
Solar power meter	$\pm 10 \text{ W/m}^2$	0 – 1370 w/m^2	5.77 W/m^2
Anemometer	$\pm 0.2 \text{ m/s}$	0 – 89 m/s	0.115 m/s
Weight balanced devise	$\pm 0.1\text{g}$	0 – 10 kg	0.05 g

3. Experimental Procedures

Providing water is the initial stage of the experimental procedure. The water will be conveyed from the feeder tank to the basin via a plastic pipe located 1 cm over the surface of the absorbing base. This will act as a level indicator. Once the fluid in the basin attains the lowest point of the feeding pipe, it is necessary to cease the flow. The feeding will resume after the process of evaporation commences and when the water level falls. The radiation transiting through the transparent cover and water will raise the temperature of the basin plate. Vapor is naturally generated and travels towards the internal surface of the transparent cover. When water vapor meets glass, it condenses and creates water drops. Drops fall along the cover as it inclines towards a collecting channel. When utilizing a traditional single-slope solar still, the feed water temperature remains neutral, but with the addition of a magnetic field, the evaporation rate will increase because of the presence of magnets, and they also act as heat storage materials and increase the absorption area. Using an exterior condenser improves the condensation process by augmenting the accessible surface area for condensation. The vapor is generated in the solar still once solar radiation heated the water in this system. The vapor is then directed into the cylindrical condensers. The vapor undergoes condensation on the inside surface of the cylindrical condenser. The water collection channel sent the condensed water to the pure water collector via plastic pipes. The air drawn within the condenser to cool it may be used as heated air for domestic applications.

3.1 Efficiency

The still efficiency can be determined by employing the following approach [21].

$$\eta = \frac{\sum m \cdot h_{fg} \cdot 1000}{A \cdot I_s \cdot 3600} \quad (2)$$

where;

m: water yield in kilograms per hour

hfg: water's latent heat is measured in kilojoules per kilogram (kJ/kg)

A: Optimal sunlight absorption surface area

Is: Hourly solar rays measured in watts per square meter (W/m²)

3.2 Performance Enhancement

A crucial determinant that shows the improvement of work in the solar distiller is the outcome of the distiller, and based on this, it can be calculated from the following equation [22].

$$\text{Improvement \%} = \frac{m_{MSS} - m_{CSS}}{m_{CSS}} \quad (3)$$

3.3 Exergy Analysis of Solar Still

The exergy analysis of the still is conducted by applying the governing equations derived from the fundamental principles of the second law of thermodynamics. Consequently, the exergy balance can be expressed in the following way [23].

$$E_{x,dest} = E_{x,in} + E_{x,out} \quad (4)$$

$$E_{x,in} = E_{x,sun} = I_t A_b \left[1 + \frac{4}{3} \left(\frac{T_{amb}+273.16}{T_{sun}} \right) - \frac{1}{3} \left(\frac{T_{amb}+273.16}{T_{sun}} \right)^4 \right] \quad (5)$$

$$E_{x,out} = E_{x,evap} = \frac{m_{evap} h_{fg}}{3600} \left[1 - \left(\frac{T_{amb}+273.16}{T_{w,b}} \right) \right] \quad (6)$$

$$h_{fg} = 2.4935 * 10^6 * (1 - 9.4779 * 10^{-4} * T_{w,b} + 1.3132 * 10^{-7} * T_{w,b}^2 - 4.7974 * 10^{-9} T_{w,b}^3) \quad (7)$$

where:

I_t : The solar energy that drops on the glass covering of the stills

A_b : The still's basin area

T_{sun} : The temperature of the Sun taken as 6000 K

h_{fg} : The vaporization Latent heat

m_{evap} : The amount of evaporation water

$T_{w,b}$: The water's temperature

The exergy efficiency is determined by dividing the output of the still by its input, and can be mathematically represented as follows [23]:

$$\eta_{EX} = \frac{E_{x,out}}{E_{x,in}} = \frac{E_{x,evap}}{E_{x,sun}} \quad (8)$$

4. Result and Discussion

The experimentation was conducted on 2 may 2024, from 8 am to 17 pm. Figure 5 illustrates the temporal changes in input parameters, including sun intensity, wind velocity, and ambient temperature. The value of solar radiation increases gradually until it reaches its maximum around 13:00 PM. Subsequently, it steadily diminishes until it reaches its minimal point. Additionally, the graphic clearly illustrates that the patterns of radiation correspond with the patterns of ambient temperature. The wind velocity gradually rises until it reaches its peak temperature at 13 p.m., and then it keeps going up and down until 17 p.m. in the evening.

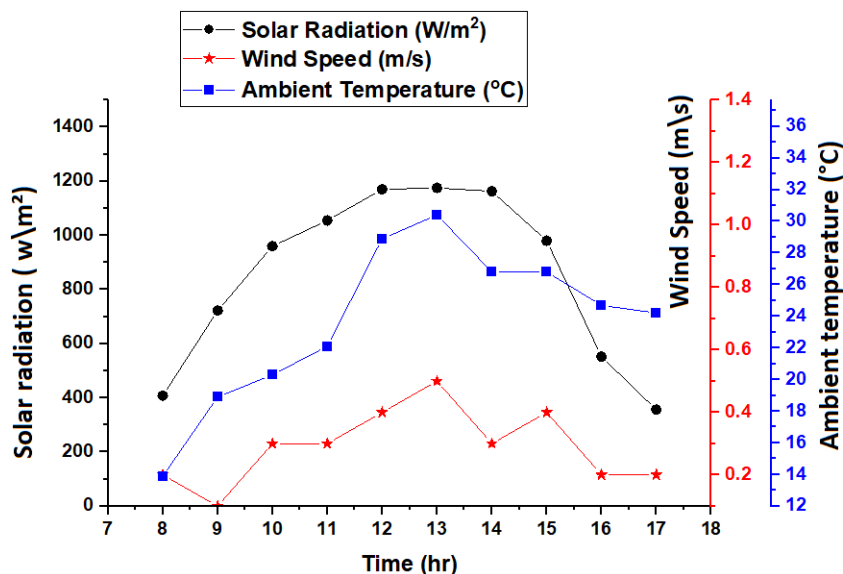


Fig. 5. Average variance in sunlight intensity, ambient temperature and wind speed throughout the experiment's day

Figure 6, Figure 7 and Figure 8 display the temperature fluctuations of the for CSS-MAG, CSS-MACO and CSS. The figure clearly shows that the temperatures rise with time and reach their highest values (77.8, 79.85, 79.66.2, 67.8) for the absorbing plate, basin water, vapor, both the out and interior surface of the transparent cover of the CSS-MAG and (77.6, 76.4, 74.1, 66.3, 67.8, 51.5, 42.5 °C) for the absorbing plate, basin water, vapor, both the out and inside glass covering surfaces, inner and vent holes of the condenser respectively of the CSS-MACO and (74, 71.7, 74.75, 67.1, 68.2 °C))respectively for the absorbing plate, basin water, vapor, both the outer and inner covering of glass surfaces of the CSS around 13:00 P.M. After that, the temperatures progressively decline in accordance with the pattern of solar radiation. The inner surface temperature of the CSS-MACO glass cover is lower compared to that of the conventional one. Since a fraction of the vapor is removed to the external condenser.

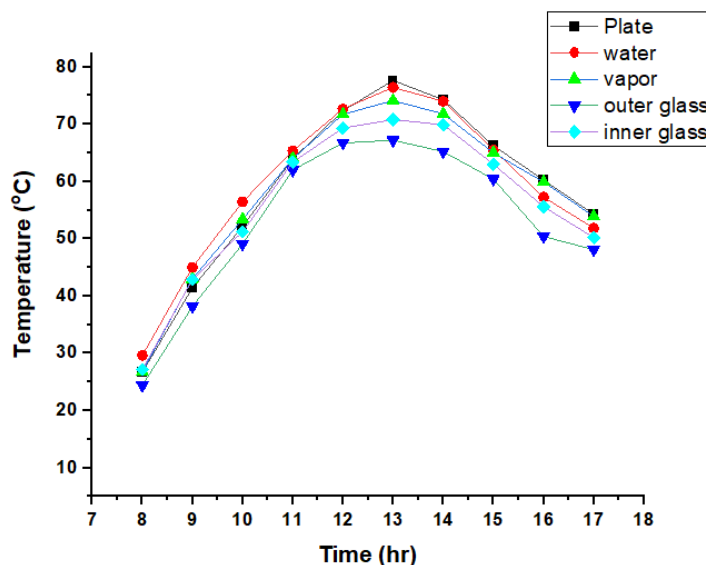


Fig. 6. Fluctuations in temperature across time was observed throughout the entirety period of the inquiry for CSS

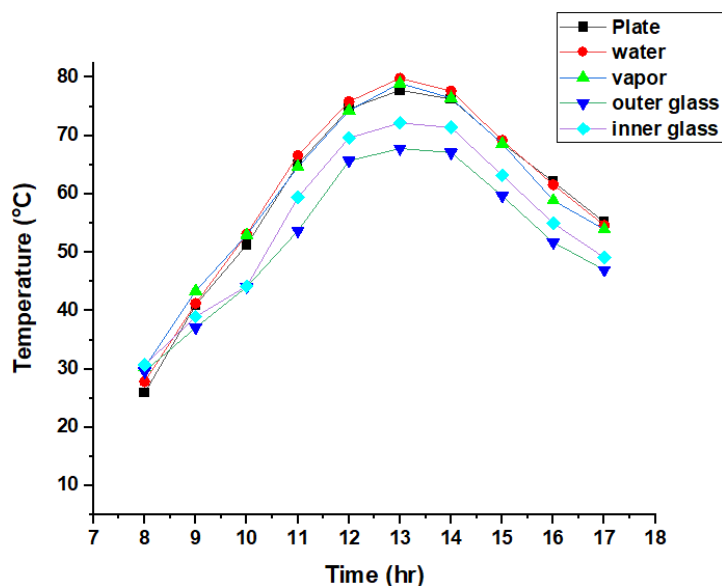


Fig. 7. Fluctuations in temperature across time was observed throughout the entirety period of the inquiry for CSS MAG

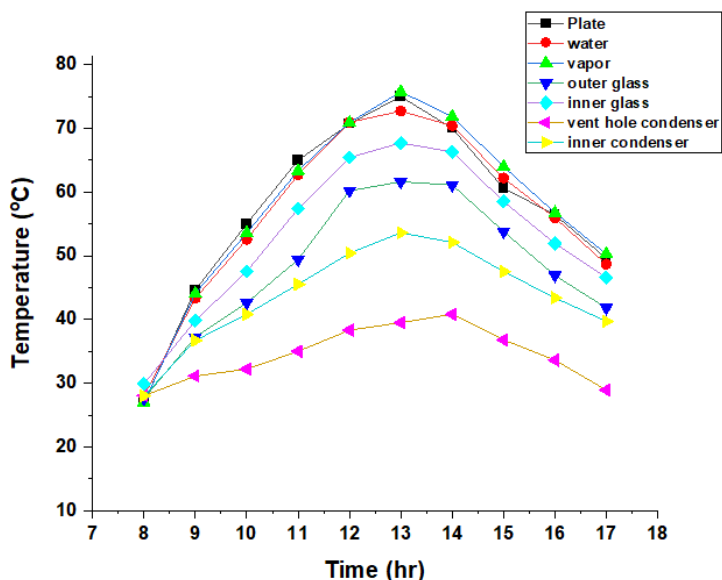


Fig. 8. Fluctuations in temperature across time was observed throughout the entirety period of the inquiry for CSS-MACO

Figure 9 displays the variation in temperature ($T_w - T_g$, in) between the internal surface of the transparent cover and the water in the basin of still throughout the experiment. The figure clearly indicates that the modified solar stills function with a bigger temperature differential compared to the CSS. We prioritize the modified solar stills to optimize their effectiveness and productivity. The key determinant of the increase in still yield is the variance in temperature between the internal surface of the covering glass and the water in the basin. The increase in this differential results in increased production due to the improved condensation and evaporation processes within the stills.

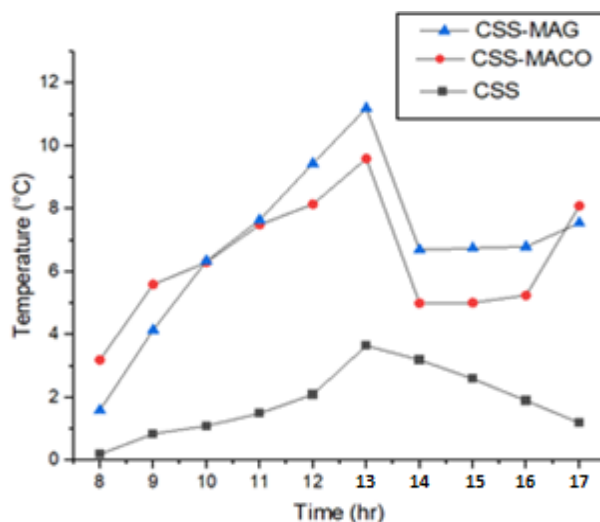


Fig. 9. Relationship between the temperature difference ($T_w - T_{g,in}$) for CSS, CSS-MAG and CSS-MACO

During the performed experimentation, it was seen that the CSS-MAG and CSS-MACO demonstrated a higher production, surpassing the standard system by a 52.63% and 37.10%, respectively. Figure 10 illustrates the overall productivity of the CSS. The production rate is 5.8, 5.2, 10, 3.8 liters per square meter per day, respectively, for CSS-MAG, CSS-MACO, and CSS.

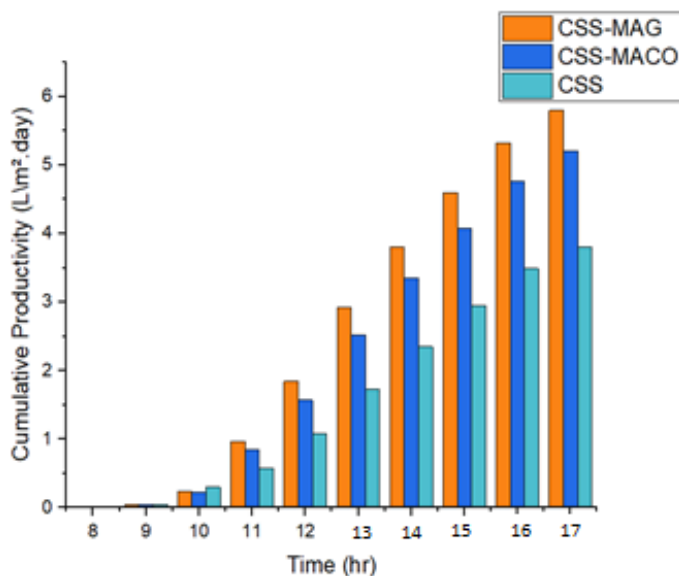


Fig. 10. Cumulative productivity for MSS and CSS

The external condenser performs a portion of the condensing process internally. When a certain amount of vapor is taken out, the lowers of the internal surface temperature of the glass cover, causing a greater variation in temperature between the basin's water and the internal surface of transparent cover. As a result, there is an increased level of condensation. In addition, the rate of evaporation increases when a portion of the vapor is eliminated. The absorber plate absorbs additional incident radiation. Consequently, extracting a portion of the vapor to the condenser, the rates of condensation and evaporation are increased. Condensation occurred in both the exterior condenser and the still. The presence of magnets inside the solar still enhances the extent of the exposed surface area available for evaporation in addition to its function as a heat storage medium,

which improves the evaporation process inside the still. What is observed from Figure 9 regarding the decrease in the productivity of the still as a result of using the magnet and the external condenser together for this design in the experiment compared to the productivity of the still with the use of magnets only is due to the incompatibility of the condensation and evaporation processes inside the still for this case, as the effect of using the condenser can be negative in some cases as stated by Rahmani *et al.*, [13]. It is possible to obtain better productivity results by using magnets with other ratios to the area so that there is compatibility between the condensation and evaporation processes inside the still.

The magnetic field (MF) is a significant and contemporary approach influencing the productivity of solar stills due to its beneficial effect on the rate of water evaporation. Previous research indicate that the magnetic field enhances the partial pressure differential between water and the glass cover. The alteration transpires in the hydration shells of the saltwater, which is expected to augment the evaporation rate and raise the efficacy of the solar still. Furthermore, the magnetic field markedly lowers the surface tension of saline water, resulting in enhanced evaporation. The intensity, direction, position, and size of magnets significantly influence the rates of water evaporation and heat transmission [24,25]. The permanent magnet is the most widely recognized magnetic media, capable of retaining its magnetic properties in the absence of magnetic fields [26]. The permanent magnets serve two functions in addition to the magnetic effect: as an energy storage substance and fins that not only improves the effectiveness of the process but also boosts the solar still performance.

Figure 11 displays the observed trends in thermal efficiency for CSS-MAG, CSS-MACO and CSS during the experimental test days. The figure illustrates a gradual increase in thermal efficiency over time, The highest recorded thermal efficiency value is (69.10,96.47,99.40%) respectively for CSS-MAG, CSS-MACO and CSS which was reached at 17:00 P.M. on 2 may 2024, respectively. Also, the overall thermal efficiency for CSS during days of experiments were 45.43%, 41.25%, 29.93%, respectively for CSS-MAG, CSS-MACO and CSS on 2 MAY 2024.

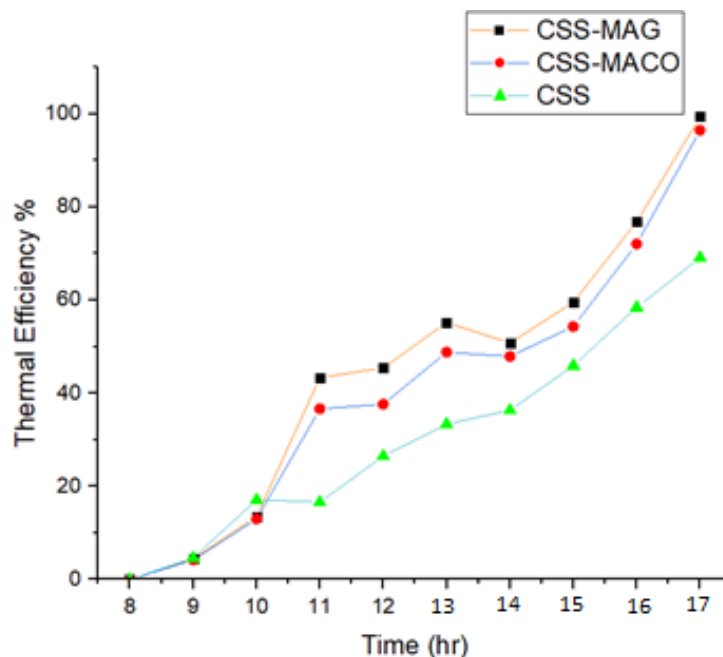


Fig. 11. Temporal fluctuations in thermal efficiency for CSS, CSS-MAG and CSS-MACO

Figure 12 shows the exergy efficiency trends observed during one of the experimental test days. The figure clearly demonstrates that the exergy efficiency progressively rises over time, peaking at 52.10% for the CSS-MAG and 46.04%, 28.84%, respectively for the CSS-MACO and CSS at 13:00 P.M.

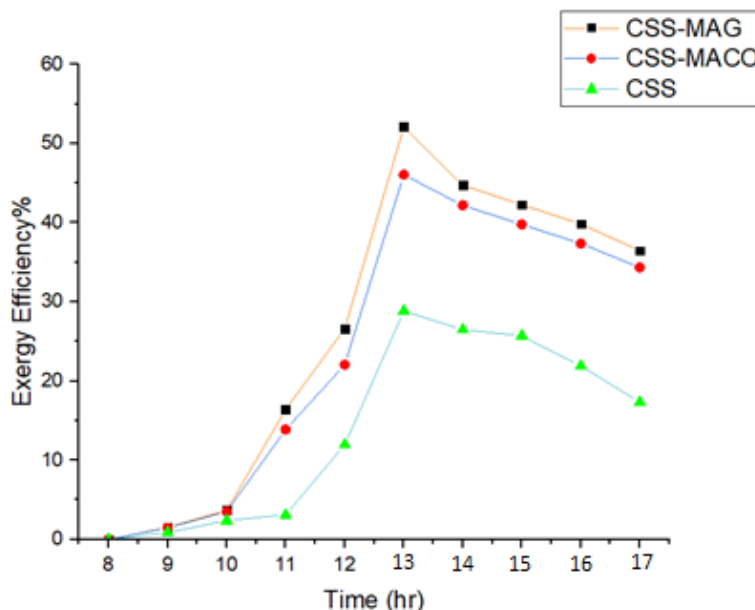


Fig. 12. Behavior of exergy efficiency along the time of experiment for CSS, CSS-MAG and CSS-MACO

5. Cost Analysis

The key prerequisites for cost analysis are the components of the still type, as indicated in Table 4 presents the cost estimation for variable as well as fixed expenses.

The cost of 1 liter from the still can be computed based on the daily accumulated yield and the remaining lifetime [27].

$$C \text{ (the yearly overall expense)} = F \text{ (fixed expense)} + V \text{ (variable expense)} \tag{9}$$

The following criteria might be considered to simplify and accomplish the cost calculation procedure.

- i. The solar still functions for a total of 325 days each year.
- ii. The duration of the still's operation is 5 years.
- iii. The change in price (V) is equivalent to 0.3 times the fixed price (F) per year, which includes the cost of maintenance.

CSS

The fixed expense of CSS is $F = 58.47\$$ per 1 m^2 , thus, from Eq. (9).

$$C = 58.47 + (0.3 \times 58.47 \times 5) = 146.175\$.$$

The general daily output of CSS is approximately $4.0375 \text{ L/m}^2 \cdot \text{day}$. Then, the output of the still during its lifespan is

$$3.8 \times 325 \times 5 = 6175 \text{L}.$$

Thus, the cost of 1 l from CSS = $146.175/6175 = 0.023\$$.

CSS-MAG

The fixed expense of CSS-MAG is $F = 62.5\$$ per 1 m^2 , thus, from Eq. (9).
 $C = 62.7 + (0.3 \times 62.7 \times 5) = 156.25\$$.

The general daily output of CSS-MAG is approximately $5.7275 \text{ L/m}^2 \cdot \text{day}$. Then, the output of the still during its lifespan is

$$5.7275 \times 325 \times 5 = 9425\text{L.}$$

Thus, the cost of 1 l from CSS-MAG = $171.25 / 9425 = 0.016\$$.

CSS-MACO

The fixed expense of CSS-MACO is $F = 69.9\$$ per 1 m^2 , thus, from Eq. (9).

$$C = 69.9 + (0.3 \times 69.9 \times 5) = 174.75\$$$

The general daily output of CSS-MACO is approximately $5.210 \text{ L/m}^2 \cdot \text{day}$. Then, the output of the still during its lifespan is $5.210 \times 325 \times 5 = 8466.25\text{L}$.

Thus, the cost of 1 l from CSS-MACO = $174.75 / 8466.25 = 0.020\$$.

Table 4
 The price of constructed solar stills

Item	Cost (\$)		
	CSS	CSS-MAG	CSS-MACO
Polystyrene container	15.27	15.27	15.27
Shaping the box with CNC machine	7.5	7.5	7.5
Iron sheet that has been galvanized	15	15	15
Paint	7.5	7.5	7.5
Glass cover	4	4	4
Plastic pipe	1	1	2
Water valve plumbing	2.2	2.2	2.2
Auxiliaries (silicon, tab, etc.)	4	4	4
Condenser	/	/	5
Water feed tank	2	2	2
Fan	/	/	0.5
Electricity cost	/	/	0.0024
Magnets	/	4	4
The total fixed cost of a 1 m^2 absorbent plate area of SSSS	58.47	62.7	69.9

A comparison of the Single Slope Solar Still performance between prior related authors' works and present is illustrated in Table 5.

Table 5
 Comparison of the present study with prior research

Authors	Date / Country	Adopted Technique	% Improvement in productivity	Productivity L/m ² .day	Cost \$/L, compared to CSS
Ahmed [14]	Summer 2012/Bahrain	CSS + passive condenser	30.0%	3.340
Rabhi <i>et al.</i> , [15]	2017/Tunisia	CSS + pin fins absorber coupled with a condenser compared	41.95%	3.492
Rahmani <i>et al.</i> , [13]	2021/Algeria	CSS + Negative effect external condenser	29% (positive effect)	3.64 (positive effect)
Dhivagar <i>et al.</i> , [17]	2022/India	CSS + rectangular magnet solar still (RMSS) SSSS + circular magnet solar still (CMSS)	(RMSS) had higher hourly productivity of about 5.8% and 13.7% than (CMSS) and (CSS), respectively	3.15 for the rectangular magnet solar still (RMSS) 2.82 for circular magnet solar still (CMSS)	RMSS is 4.5% and 22.2% lower cost than the estimated in CMSS and CSS, respectively
Rufuss <i>et al.</i> , [18]	2022/India	CSS + graphite plate	There was an overall increase of 62% and 235% in the daytime and night-time yield, respectively	5.5	3.7% cheaper than for a conventional still
Current Study	May 2024/ Iraq	CSS + magnetic field CSS + magnetic field external condenser	52.6% 37.8 %	5.8 5.21	CSS-MAG is 2% and 30.43% lower cost than CSS-MACO and CSS respectively

6. Conclusion

Three solar stills were built, each having a single slope and a single basin. Conventional and altered techniques were empirically examined at the Engineering Technical college of Najaf (32° 1' N and 44° 19' E.).

- i. The magnetic fields in CSS-MAG serve two functions in addition to the magnetic effect: heat storage and extended surfaces. These functions lead to an increase in water temperature and an accelerated rate of evaporation.
- ii. The water temperature of this still attained its highest value of 79.85°C, surpassing the temperatures of 76.4 °C and 71.7°C achieved using CSS-MACO and CSS, respectively.
- iii. An external condenser enhances the condensation process occurring inside it. When a fraction of the vapor is removed, lowers of the interior surface of translucent cover temperature, resulting in an increased temperature disparity between the internal surface of the transparent cover and the basin's water condensation in the CSS-MACO. The absorption of incoming radiation by the plate intensifies as extra vapor is evacuated to the condenser unit, in addition to presence of magnets inside the still which, elevated rate of evaporation process.
- iv. The experiment demonstrated that the modified stills produced an output 5.8, and 5.21 L/m². day for CSS-MAG and CSS-MACO, respectively which is 52.6, and 37.8 % higher than that of CSS (3.8 L\m². day).

- v. The experiments showed that the solar still with the use of magnets gave better performance than the solar still with the use of magnets and an external condenser together.
- vi. The modified stills achieved maximum exergy efficiency of 28.84%, 52.10% and 46.04% and thermal efficiency of 29.93%, 45.43% and 41.25%, for CSS, CSS-MAG and CSS-MACO, respectively.
- vii. A cost analysis was conducted to compare the expenses of stills. The modified stills remained economically efficient compared to the ordinary still.

References

- [1] Kabeel, A. E., A. Muthu Manokar, Ravishankar Sathyamurthy, D. Prince Winston, S. A. El-Agouz, and Ali J. Chamkha. "A review on different design modifications employed in inclined solar still for enhancing the productivity." *Journal of Solar Energy Engineering* 141, no. 3 (2019): 031007. <https://doi.org/10.1115/1.4041547>
- [2] Al-Abayechi, Yasir, Yaser Alaiwi, and Zainab Al-Khafaji. "Exploration of key approaches to enhance evacuated tube solar collector efficiency." *Journal of Advanced Research in Numerical Heat Transfer* 19, no. 1 (2024): 1-14. <https://doi.org/10.37934/arnht.19.1.114>
- [3] Raj, S. Varun, and A. Muthu Manokar. "Design and analysis of solar still." *Materials Today: Proceedings* 4, no. 8 (2017): 9179-9185. <https://doi.org/10.1016/j.matpr.2017.07.275>
- [4] Lal, Radha Krishna, Shubham Mishra, J. P. Dwivedi, and Harshit Dwivedi. "A comprehensive study of the different parameters of solar still." *Materials Today: Proceedings* 4, no. 2 (2017): 3572-3580. <https://doi.org/10.1016/j.matpr.2017.02.249>
- [5] Abdulridha, Hussein Oleiwi, Hassanain Ghani Hameed, and Basil Noori Merzah. "An experimental study of the performance of a finned tube solar collector on a single slope solar still." *Egyptian Journal of Petroleum* 33, no. 1 (2024): 5. <https://doi.org/10.62593/2090-2468.1010>
- [6] Kabeel, Abd Elnaby, El-Sayed El-Agouz, Muthu Manokar Athikesavan, Rajendran Duraisamy Ramalingam, Ravishankar Sathyamurthy, Nakka Prakash, and Chandran Prasad. "Comparative analysis on freshwater yield from conventional basin-type single slope solar still with cement-coated red bricks: an experimental approach." *Environmental Science and Pollution Research* 27 (2020): 32218-32228. <https://doi.org/10.1007/s11356-019-07288-z>
- [7] Hameed, Hassanain Ghani, Hayder Azeez Neamah Diabil, and M. A. Al-Moussawi. "A numerical investigation of the enhancement of single-slope single-basin solar still productivity." *Energy Reports* 9 (2023): 484-500. <https://doi.org/10.1016/j.egy.2022.11.199>
- [8] Dhivagar, R., M. Mohanraj, K. Hidouri, and Ye Belyayev. "Energy, exergy, economic and enviro-economic (4E) analysis of gravel coarse aggregate sensible heat storage-assisted single-slope solar still." *Journal of Thermal Analysis and Calorimetry* 145 (2021): 475-494. <https://doi.org/10.1007/s10973-020-09766-w>
- [9] Saeed, Muntadher Mohammed Ali, Dhafer Manea Hachim, and Hassanain Ghani Hameed. "Numerical Investigation for Single Slope Solar Still Performance with Optimal Amount of Nano-PCM." *Journal of Advanced Research in Fluid Mechanics and Thermal Sciences* 63, no. 2 (2019): 302-316.
- [10] Jaafar, Zahraa Abdulkareem, Hassanain Ghani Hameed, and Ridha Hasan Hussein. "Experimental investigation of a single slope solar still performance-evaporation process enhancement." In *IOP Conference Series: Materials Science and Engineering*, vol. 928, no. 2, p. 022096. IOP Publishing, 2020. <https://doi.org/10.1088/1757-899X/928/2/022096>
- [11] Faisal, Zahraa A., Hassanain Ghani Hameed, and Dhafer Manea H. Al-Shamkhee. "Performance enhancing of single slope solar still using glass cover cooling." In *AIP Conference Proceedings*, vol. 2710, no. 1. AIP Publishing, 2024. <https://doi.org/10.1063/5.0144511>
- [12] Al-Qasaab, Mohammed R., Qahtan A. Abed, and Wisam A. Abd Al-wahid. "Enhancement the solar distiller water by using parabolic dish collector with single slope solar still." *Journal of Thermal Engineering* 7, no. 4 (2021): 1000-1015. <https://doi.org/10.18186/thermal.931352>
- [13] Rahmani, Ahmed, Fouzia Khemmar, and Zine Saadi. "Experimental investigation on the negative effect of the external condenser on the conventional solar still performance." *Desalination* 501 (2021): 114914. <https://doi.org/10.1016/j.desal.2020.114914>
- [14] Ahmed, Husham M. "Seasonal performance evaluation of solar stills connected to passive external condensers." *Scientific Research and Essays* 7, no. 13 (2012): 1444-1460. <https://doi.org/10.5897/SRE12.177>
- [15] Rabhi, Kamel, Rached Nciri, Faouzi Nasri, Chaouki Ali, and Habib Ben Bacha. "Experimental performance analysis of a modified single-basin single-slope solar still with pin fins absorber and condenser." *Desalination* 416 (2017): 86-93. <https://doi.org/10.1016/j.desal.2017.04.023>

- [16] Holysz, Lucyna, Aleksandra Szczes, and Emil Chibowski. "Effects of a static magnetic field on water and electrolyte solutions." *Journal of Colloid and Interface Science* 316, no. 2 (2007): 996-1002. <https://doi.org/10.1016/j.jcis.2007.08.026>
- [17] Dhivagar, Ramasamy, Shreen El-Sapa, Ali Jawad Alrubaie, Ameer Al-Khaykan, Ali J. Chamkha, Hitesh Panchal, and Mahmoud S. El-Sebaey. "A case study on thermal performance analysis of a solar still basin employing ceramic magnets." *Case Studies in Thermal Engineering* 39 (2022): 102402. <https://doi.org/10.1016/j.csite.2022.102402>
- [18] Rufuss, D. Dsilva Winfred, S. Arulvel, V. Anil Kumar, P. A. Davies, T. Arunkumar, Ravishankar Sathyamurthy, A. E. Kabeel et al. "Combined effects of composite thermal energy storage and magnetic field to enhance productivity in solar desalination." *Renewable Energy* 181 (2022): 219-234. <https://doi.org/10.1016/j.renene.2021.07.124>
- [19] Zaraa Allah, Mohammad, Azian Hariri, and Haslinda Mohamed Kamar. "Comparison of Thermal Comfort Condition of Naturally Conditioned Semi-Outdoor, Courtyard and Indoor Air-Conditioned Spaces in Tropical Climate." *Semarak Engineering Journal* 1, no. 1 (2023): 10-15.
- [20] Dumka, Pankaj, and Dhananjay R. Mishra. "Performance evaluation of single slope solar still augmented with the ultrasonic fogger." *Energy* 190 (2020): 116398. <https://doi.org/10.1016/j.energy.2019.116398>
- [21] Rajaseenivasan, T., P. Nelson Raja, and K. Srithar. "An experimental investigation on a solar still with an integrated flat plate collector." *Desalination* 347 (2014): 131-137. <https://doi.org/10.1016/j.desal.2014.05.029>
- [22] Hussien, Hasanen M., M. M. Younes, Wissam H. Alawee, A. S. Abdullah, Suha A. Mohammed, T. E. M. Atteya, Faheem Abbas, and Z. M. Omara. "An experimental comparison study between four different designs of solar stills." *Case Studies in Thermal Engineering* 44 (2023): 102841. <https://doi.org/10.1016/j.csite.2023.102841>
- [23] Khafaji, Hayder Q. A., Hasanain A. Abdul Wahhab, Wisam Abed Kattea Al-Maliki, Falah Alobaid, and Bernd Epple. "Energy and exergy analysis for single slope passive solar still with different water depth located in Baghdad center." *Applied Sciences* 12, no. 17 (2022): 8561. <https://doi.org/10.3390/app12178561>
- [24] Alawee, Wissam H., Karrar A Hammoodi, Hayder A. Dhahad, Z. M. Omara, Fadl A. Essa, A. S. Abdullah, and M. I. Amro. "Effects of magnetic field on the performance of solar distillers: a review study." *Engineering and Technology Journal* 41, no. 1 (2023): 121-131. <https://doi.org/10.30684/etj.2022.134576.1240>
- [25] Yehia, Ahmed, Hesham Abdel-Ma'ouz, Ahmed Mostafa, Hassan Mohamed, and Mohamed Sayed. "Modelling and Analysis of Evacuated Tube Solar Collector Working with Hybrid Nanofluid." *Journal of Advanced Research in Numerical Heat Transfer* 23, no. 1 (2024): 88-96. <https://doi.org/10.37934/arnht.23.1.8896>
- [26] Rasli, Nur Ain Shafiqah, and Nur Azmah Nordin. "Synthesization and characterization of dual properties of nickel zinc ferrite for magnetorheological materials." *Journal of Advanced Research Design* 95, no. 1 (2022): 1-11.
- [27] Abdullah, A. S., Z. M. Omara, A. Alarjani, and F. A. Essa. "Experimental investigation of a new design of drum solar still with reflectors under different conditions." *Case Studies in Thermal Engineering* 24 (2021): 100850. <https://doi.org/10.1016/j.csite.2021.100850>